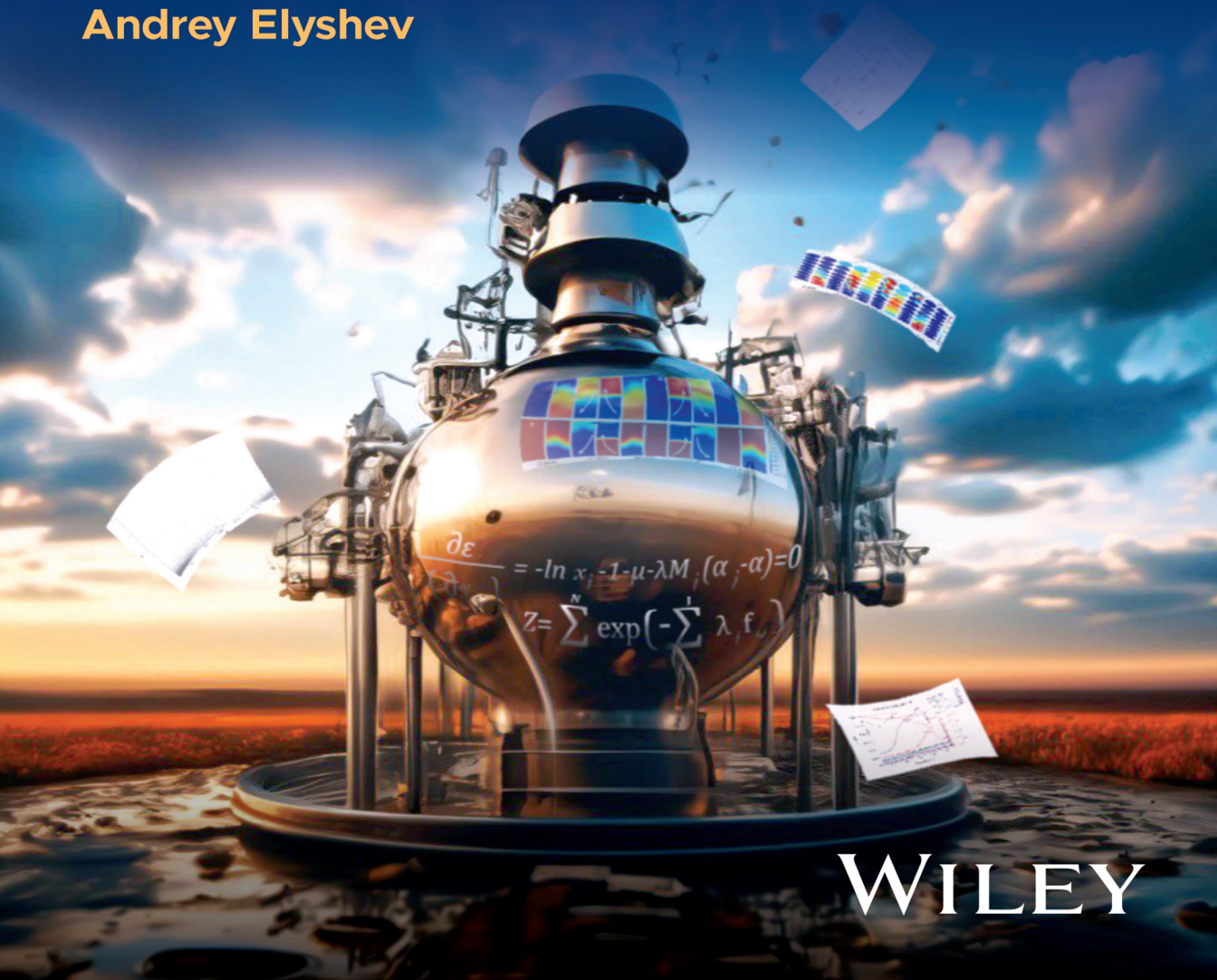


# Mathematical Modeling of Complex Reaction Systems in the Oil and Gas Industry

Edited by

Jorge Ancheyta • Andrey Zagoruiko  
Andrey Elyshev



WILEY



**Mathematical Modeling of Complex  
Reaction Systems in the Oil and  
Gas Industry**



# Mathematical Modeling of Complex Reaction Systems in the Oil and Gas Industry

Edited by

*Jorge Ancheyta*

*Instituto Mexicano del Petróleo  
Mexico City, Mexico*

*Andrey Zagoruiko*

*Borshkov Institute of Catalysis  
Novosibirsk, Russia*

*Andrey Elyshev*

*University of Tyumen  
Tyumen, Russia*

**WILEY**

This edition first published 2024  
© 2024 John Wiley & Sons Ltd

All rights reserved, including rights for text and data mining and training of artificial intelligence technologies or similar technologies. No part of this publication may be reproduced, stored in a retrieval system, or transmitted, in any form or by any means, electronic, mechanical, photocopying, recording or otherwise, except as permitted by law. Advice on how to obtain permission to reuse material from this title is available at <http://www.wiley.com/go/permissions>.

The right of Andrey Elyshev, Andrey Zagoruiko, and Jorge Ancheyta to be identified as the authors of the editorial material in this work has been asserted in accordance with law.

#### *Registered Offices*

John Wiley & Sons, Inc., 111 River Street, Hoboken, NJ 07030, USA  
John Wiley & Sons Ltd, The Atrium, Southern Gate, Chichester, West Sussex, PO19 8SQ, UK

For details of our global editorial offices, customer services, and more information about Wiley products visit us at [www.wiley.com](http://www.wiley.com).

Wiley also publishes its books in a variety of electronic formats and by print-on-demand. Some content that appears in standard print versions of this book may not be available in other formats.

Trademarks: Wiley and the Wiley logo are trademarks or registered trademarks of John Wiley & Sons, Inc. and/or its affiliates in the United States and other countries and may not be used without written permission. All other trademarks are the property of their respective owners. John Wiley & Sons, Inc. is not associated with any product or vendor mentioned in this book.

#### *Limit of Liability/Disclaimer of Warranty*

While the publisher and authors have used their best efforts in preparing this work, they make no representations or warranties with respect to the accuracy or completeness of the contents of this work and specifically disclaim all warranties, including without limitation any implied warranties of merchantability or fitness for a particular purpose. No warranty may be created or extended by sales representatives, written sales materials or promotional statements for this work. This work is sold with the understanding that the publisher is not engaged in rendering professional services. The advice and strategies contained herein may not be suitable for your situation. You should consult with a specialist where appropriate. The fact that an organization, website, or product is referred to in this work as a citation and/or potential source of further information does not mean that the publisher and authors endorse the information or services the organization, website, or product may provide or recommendations it may make. Further, readers should be aware that websites listed in this work may have changed or disappeared between when this work was written and when it is read. Neither the publisher nor authors shall be liable for any loss of profit or any other commercial damages, including but not limited to special, incidental, consequential, or other damages.

*Library of Congress Cataloging-in-Publication Data is Applied for*  
Hardback ISBN: 9781394220021

Cover Design: Wiley

Cover Image: © Created and Designed by Darya Obanina together with the Shdevrum neural network

Set in 9.5/12.5pt STIXTwoText by Straive, Pondicherry, India

## Contents

**List of Contributors** *xiii*

**Preface** *xv*

- 1 Modeling the Kinetics of Hydrocracking of Heavy Oil with Mineral Catalyst** *1*  
*Guillermo Félix, Fernando Trejo, and Jorge Ancheyta*
- 1.1 Introduction *1*
- 1.1.1 Reserves and Production of Heavy Crude Oils *1*
- 1.1.2 Heavy Crude Oil Upgrading Processes *2*
- 1.1.3 Reactions During Slurry Phase Hydrocracking *6*
- 1.1.4 Catalysts for Hydrocracking of Heavy Crude Oils in Slurry Phase *6*
- 1.2 Kinetic Models *7*
- 1.2.1 General Types of Kinetic Models *8*
- 1.2.1.1 Lumping Kinetic Models *8*
- 1.2.1.2 Continuous Lumping Kinetic Models *8*
- 1.2.1.3 Single-Event Kinetic Models *10*
- 1.2.2 Kinetic Models Reported in the Literature for Hydrocracking of Heavy Crude Oils Using Dispersed Catalysts *10*
- 1.2.2.1 Kinetic Models Based on Distillation Curves *10*
- 1.2.2.2 Kinetic Models Based on SARA Fractions *18*
- 1.2.3 Kinetic Models Based on Continuous Lumping *21*
- 1.2.4 Thermodynamic Model to Predict the Asphaltenes Flocculation and Sediments Formation *22*
- 1.3 Kinetic Parameters Estimation *24*
- 1.3.1 Assumptions *26*
- 1.3.2 Initialization of Parameters *27*
- 1.3.3 Nonlinear Optimization *28*
- 1.3.4 Objective Function *28*
- 1.3.5 Sensitivity and Statistical Analyses *29*
- 1.3.5.1 Perturbations *29*
- 1.3.5.2 Parity Plots *29*
- 1.3.5.3 Residuals *29*
- 1.3.5.4 AIC and BIC *30*
- 1.4 Results and Discussion *30*
- 1.4.1 Kinetic Parameters *30*

1.4.1.1	Assumptions	30
1.4.1.2	Reaction Rate Coefficients	32
1.4.1.3	Activation Energies	38
1.4.2	Accuracy of the Kinetic Models	38
1.4.2.1	SARA-Based Models	38
1.4.2.2	Distillation Curves-Based Models	41
1.4.3	Reactions in Parallel and in Series	44
1.4.4	Thermodynamic Model	45
1.4.5	General Comments	48
1.5	Conclusion	50
	References	50
<b>2</b>	<b>Modeling Catalyst Deactivation of Hydrotreating of Heavy Oils</b>	<b>56</b>
	<i>Javier Jurado, Vicente Samano, and Jorge Ancheyta</i>	
2.1	Introduction	56
2.2	Mechanisms of Deactivation	57
2.2.1	Coking Deposition (Fouling)	59
2.2.2	Metal Deposition (Poisoning)	59
2.3	Deactivation Models	60
2.3.1	Deactivation Models by Coke Deposition	60
2.3.2	Deactivation Models by Metal Deposition	65
2.3.3	Deactivation Models by Coke and Metal Deposition	70
2.4	Development of Models for HDT Catalyst Deactivation	78
2.4.1	Important Issues	78
2.4.2	Final Remarks	82
2.5	Development of a Reactor Model for Heavy Oil Hydrotreating with Catalyst Deactivation Based on Vanadium and Coke Deposition	83
2.5.1	The Model	84
2.5.1.1	Description	84
2.5.1.2	Solution of the Model	86
2.5.1.3	Advantages of the Model	86
2.5.1.4	Procedure for Parameter Estimation	88
2.5.2	Results and Discussion	89
2.5.2.1	Profiles of Sulfur and Vanadium Concentration in Products	89
2.5.2.2	Comparison of Predictions with Literature and Proposed Model	90
2.5.2.3	Profiles of Coke and Vanadium on Catalyst	91
2.5.2.4	Final Remarks	93
2.5.3	Usefulness of the Model	95
2.5.4	Conclusion	96
2.6	Application of the Deactivation Model for Hydrotreating of Heavy Crude Oil in Bench-Scale Reactor	96
2.6.1	Properties of Heavy Oil	96
2.6.2	Properties of the Catalyst	96
2.6.3	Bench-Scale Reactor	98
2.6.4	Catalyst Activation	98
2.6.5	Operating Conditions	99
2.6.6	Characterization Methods	99

- 2.6.7 Parameter Estimation 100
- 2.6.8 Results and Discussion 101
- 2.6.8.1 Evolution of Sulfur and Metals Concentration in Products 101
- 2.6.8.2 Coke and Metals on Catalyst 102
- 2.6.9 Conclusion 105
- Nomenclature 105
- References 111

### **3 Simulation of the Oxidative Regeneration of Coked Catalysts: Kinetics, Catalyst Pellet, and Bed Levels 116**

*Sergey Zazhigalov, Osman Abdulla, and Andrey Zagoruiko*

- 3.1 Introduction 116
- 3.2 Process Chemistry and Laboratory Experiments 117
- 3.2.1 Catalyst and Proposed Reactions 117
- 3.2.2 Reaction Kinetics 119
- 3.2.3 Experimental Setup 121
- 3.2.4 Experiments 124
- 3.3 Mathematical Model 126
- 3.4 Model Solution Method 132
- 3.5 Modeling Results 133
- 3.6 Conclusion 134
- 3.7 Notation 136
- Abbreviations 136
- Acknowledgment 137
- References 137

### **4 Modeling of Unsteady-State Catalytic and Adsorption–Catalytic Processes: Novel Reactor Designs 138**

*Sergey Zazhigalov, Andrey Elyshev, and Andrey Zagoruiko*

- 4.1 Introduction 138
- 4.2 Novel Reactor Designs for Catalytic Reverse-Flow and Adsorption–Catalytic Processes 141
- 4.2.1 Unsteady-State Catalytic Reverse-Flow Process 141
- 4.2.2 Adsorption–Catalytic Process 142
- 4.3 Mathematical Models of the Processes 145
- 4.3.1 Unsteady-State Catalytic Reverse-Flow Process 145
- 4.3.2 Adsorption–Catalytic Process 146
- 4.4 Results 148
- 4.4.1 Unsteady-State Catalytic Reverse-Flow Process 148
- 4.4.2 Adsorption–Catalytic Process 153
- 4.4.2.1 Reactor with Truncated Cone Entrance 153
- 4.4.2.2 Multisectional Reactor 156
- 4.5 Conclusion 164
- 4.6 Notation 165
- Abbreviations 165
- Acknowledgments 165
- References 166

- 5 Molecular Reconstruction of Complex Hydrocarbon Mixtures for Modeling of Heavy Oil Processing 168**  
*Nikita Glazov and Andrey Zagoruiko*
- 5.1 Introduction 168
  - 5.2 The Problem 168
  - 5.3 Illustration 169
  - 5.4 Reconstruction by Entropy Maximization (REM) 169
  - 5.5 Stochastic Reconstruction (SR) 174
  - 5.6 SR-EM 179
  - 5.7 Structure-Oriented Lumping (SOL) Method 181
  - 5.8 State Space Representation Method 182
  - 5.9 Molecular Type-Homologous Series Matrix 183
  - 5.10 Conclusion 184
  - Acknowledgment 184
  - References 184
- 6 Modeling of Catalytic Hydrotreating Reactor for Production of Green Diesel 187**  
*Alexis Tirado, Fernando Trejo, and Jorge Ancheyta*
- 6.1 Introduction 187
  - 6.2 Conversion of Vegetable Oils into Renewable Fuels 187
  - 6.2.1 Commercial Production of Renewable Diesel 189
  - 6.3 Hydrotreating Kinetic Models and Reaction Pathways 190
  - 6.3.1 Model Compounds 190
  - 6.3.2 Vegetable Oils 197
  - 6.4 Models for Catalytic Deactivation 204
  - 6.5 Reactor Modeling for Vegetable Oil Hydrotreating 205
  - 6.5.1 Deviation from Ideal Flow Pattern 208
  - 6.6 The Importance of Modelling Reactors for Vegetable Oil Hydrotreating 210
  - 6.7 Study Case for the Development of Dynamic Reactor Model 210
  - 6.7.1 Equations and Assumptions for Hydrotreating Reactor Modeling 210
  - 6.7.2 Kinetic Model for Hydrotreating of Vegetable Oil 213
  - 6.7.3 Hydrogen Consumption and Gas Generation 213
  - 6.7.4 Solution of Reactor Models 215
  - 6.8 Analysis and Discussion of Results 217
  - 6.8.1 Criteria to Ensure Ideal Behaviors in Trickle-Bed Reactor 217
  - 6.8.2 Dynamic Profiles of Feedstock and Products of a Bench-Scale Reactor for Catalytic Hydrotreating of Vegetable Oil 219
  - 6.8.3 Validation of Hydrotreating Reactor Model with Pilot Plant Data 222
  - 6.8.4 Dynamic Simulation of a Non-isothermal Reactor 225
  - 6.8.4.1 Comparison of Non-isothermal Model with Experimental Results in Isothermal Reactor 225
  - 6.8.4.2 Comparison of Bench-Scale and Pilot-Scale Reactor Under Non-isothermal Operating Condition 227
  - 6.8.5 Dynamic Simulation of an Adiabatic Commercial Reactor 229
  - 6.8.5.1 Configuration of Hydrogen Quenching 232
  - 6.8.5.2 Liquid-Phase Yields and Gas Composition 232
  - 6.9 Conclusions 235
  - References 236

<b>7</b>	<b>Modeling of Slurry-Phase Hydrocracking Reactor</b>	<b>242</b>
	<i>Cristian Calderón and Jorge Ancheyta</i>	
7.1	Introduction	242
7.1.1	Characteristics of Slurry-Phase Reactors for Hydrocracking	242
7.1.1.1	Type of Reactors	242
7.1.1.2	Catalyst Properties	245
7.1.2	SPR Modeling	246
7.1.2.1	Classification	246
7.1.2.2	Model Complexity	249
7.1.2.3	Models for Slurry Reactors	249
7.2	Proposed Generalized Model	253
7.2.1	Equations for the Generalized Model	253
7.2.2	Solids Concentration	257
7.2.3	Initial and Boundary Conditions	257
7.2.4	Estimation of Model Parameters	260
7.2.5	Gas Holdup	260
7.2.6	Gas-Liquid Mass Transfer Coefficients	262
7.2.7	Gas-Liquid Equilibrium	264
7.2.8	Liquid-Solid and Gas-Solid Mass Transfer Coefficients	264
7.2.9	Dispersion Coefficients	265
7.2.10	Heat Transfer Coefficients	267
7.2.11	Example of Simplification of the Generalized Model	267
7.3	Simplified Models	268
7.3.1	SPR 1D Model	268
7.3.2	SPR 2D Model	269
7.3.3	Continuous Stirred Tank Reactor Model	270
7.3.4	Parameters	270
7.3.5	Reaction Kinetics	273
7.3.6	Solution Method	274
7.4	Numerical Simulations	275
7.4.1	Experimental Reactors	275
7.4.1.1	Dynamic Simulations of CSTR and SPR	275
7.4.1.2	Steady-State Simulations of a SPR	278
7.4.2	Industrial-Scale Reactor	280
7.4.2.1	Dynamic Simulations of the Industrial Slurry-Phase Reactor	283
7.4.2.2	Sensitivity Analysis for the Industrial Slurry-Phase Reactor	287
7.5	Conclusions	291
	Nomenclature	294
	References	297
<b>8</b>	<b>Modeling of Fischer-Tropsch Synthesis Reactor</b>	<b>303</b>
	<i>César I. Méndez and Jorge Ancheyta</i>	
8.1	Fundamentals of the Fischer-Tropsch Synthesis to Produce Clean Fuels	303
8.1.1	Fischer-Tropsch Synthesis Technology	304
8.1.2	Fischer-Tropsch Synthesis Catalysts	307
8.1.2.1	Cobalt-Based Catalysts	307
8.1.2.2	Iron-Based Catalysts	308
8.1.2.3	Catalyst Support	309

- 8.1.3 Fischer–Tropsch Synthesis Kinetic Models 309
  - 8.1.3.1 Kinetic Models Developed with Iron Catalyst 310
  - 8.1.3.2 Kinetic Models Developed with Cobalt Catalyst 310
- 8.1.4 General Aspects of Fischer–Tropsch Catalytic Mechanisms 315
- 8.1.5 The Fischer–Tropsch Synthesis Product Distribution Models 321
- 8.1.6 Final Remarks 324
- 8.2 Modeling of Catalytic Fixed-Bed Reactors for Fuels Production by Fischer–Tropsch Synthesis 324
  - 8.2.1 Introduction 324
  - 8.2.2 Modeling of Fixed-Bed Fischer–Tropsch Reactors 324
    - 8.2.2.1 Classification of Fixed-Bed Fischer–Tropsch Reactor Models 325
    - 8.2.2.2 One- and Two-Dimensional Pseudohomogeneous Model 325
    - 8.2.2.3 One- and Two-Dimensional Heterogeneous Model 326
  - 8.2.3 Development of a Generalized Fixed-Bed Fischer–Tropsch Reactor Model 326
    - 8.2.3.1 General Equations of the Model 326
    - 8.2.3.2 Boundary Conditions of the Proposed Generalized Model 334
    - 8.2.3.3 Pressure Drop 337
  - 8.2.4 Model Parameters 340
    - 8.2.4.1 Mass Transfer Parameters 340
    - 8.2.4.2 Heat Transfer Parameters 341
    - 8.2.4.3 Phase Equilibrium 343
    - 8.2.4.4 Catalyst Particles Parameters 345
    - 8.2.4.5 Catalytic Bed Parameters 352
  - 8.2.5 Final Remarks 354
- 8.3 Importance of Proper Hydrodynamics Modeling in Fixed-Bed Fischer–Tropsch Synthesis Reactor 354
  - 8.3.1 Introduction 354
  - 8.3.2 Mathematical Modeling of the Fixed-Bed Fischer–Tropsch Synthesis Reactor 354
    - 8.3.2.1 Reactor Model 355
    - 8.3.2.2 Kinetics 356
    - 8.3.2.3 Other Parameters and Correlations 357
    - 8.3.2.4 Numerical Method 357
  - 8.3.3 Results and Discussion 358
    - 8.3.3.1 Simulations for the One-Stage Reactor 358
    - 8.3.3.2 Simulations for the Two-Stage Reactor 364
  - 8.3.4 Final Remarks 371
- 8.4 Dynamic One-Dimensional Pseudohomogeneous Model for Fischer–Tropsch Reactors 371
  - 8.4.1 Introduction 371
  - 8.4.2 Formulation of the Model 371
    - 8.4.2.1 Model Equations and Solution 371
    - 8.4.2.2 Model Parameters, Correlations, and Kinetics 372
  - 8.4.3 Results and Discussion 373
    - 8.4.3.1 Experimental Data 373
    - 8.4.3.2 Conversion of CO and H<sub>2</sub> 373
    - 8.4.3.3 Temperature Profiles 378
  - 8.4.4 Product’s selectivity 381

8.4.5	Final Remarks	388
8.5	Modeling and Control of a Fischer–Tropsch Synthesis Reactor with a Novel Mechanistic Kinetic Approach	390
8.5.1	Introduction	390
8.5.2	Formulation of the Model	392
8.5.2.1	Model Equations and Solution	392
8.5.2.2	Model Parameters and Correlations	394
8.5.2.3	The Mechanistic FTS Kinetic Model	395
8.5.3	Implementation of the PI Controller	396
8.5.4	Results and Discussion	397
8.5.4.1	Experimental Data	397
8.5.4.2	Simulations of the Syngas Conversion, Light Gases, and Heavy Liquid Selectivity	397
8.5.4.3	Simulations of the Fischer–Tropsch Fixed-Bed Reactor and the Cooling Jacket Thermal Behavior	404
8.5.4.4	Surfaces of the Syngas Conversion and the Heavy Liquids Selectivity as a Function of the FTS Reactor Temperature	405
8.5.5	Final Remarks	408
8.6	On the use of Steady-State Optimal Initial Operating Conditions for the Control Scheme Implementation of a Fixed-Bed Fischer–Tropsch Reactor	408
8.6.1	Introduction	408
8.6.2	Methodology	408
8.6.2.1	Model Equations and Numerical Solution	408
8.6.2.2	Model Parameters, Correlations, and Kinetics	409
8.6.2.3	Steady-State Nonlinear Constrained Optimization Problem	409
8.6.2.4	Implementation of the Control Scheme	413
8.6.3	Results and discussion	414
8.6.3.1	Experimental Data	414
8.6.3.2	Simulations of the Steady-State Nonlinear Constrained Optimization Problem: CO Conversion, $S_{C_{5+}}$ Selectivity, and Temperature Profiles	415
8.6.3.3	Simulations of the Control Scheme Implementation: CO Conversion, $S_{C_{5+}}$ Selectivity, and Temperature Profiles	416
8.6.4	Final Remarks	420
	References	421
<b>9</b>	<b>Computational Fluid Dynamics Modeling of Mass Transfer Processes in Structured Beds of Microfibrous Catalysts</b>	<b>434</b>
	<i>Sergey Lopatin, Andrey Elyshev, and Andrey Zagoruiko</i>	
9.1	Introduction	434
9.2	Mathematical Model	436
9.2.1	Model Description	437
9.2.2	Computing Domain	437
9.2.3	Simulation Object Geometry	437
9.2.4	Reaction	439
9.2.5	Model Parameters	440
9.3	Simulation Results	440
9.3.1	Cartridge Channel with Corrugated Structuring Mesh	440

- 9.3.2 Influence of GFC Textile Shape 443
- 9.3.3 Cartridge Channel Without Corrugated Structuring Mesh 443
- 9.3.4 Two-Sided Washing of GFC Textiles 447
- 9.3.5 Convective Flow Inside the GFC Thread 449
- 9.3.6 The General Description of Mass Transfer in GFC 451
- 9.4 Conclusion 452
- Abbreviations 453
- Acknowledgement 453
- References 453

**Index** 456

## List of Contributors

**Osman Abdulla**

Tyumen State University, Tyumen, Russia

**Jorge Ancheyta**

Department of Petroleum Engineering  
Kazan Federal University, Kazan, Russia;  
Instituto Mexicano del Petróleo  
Mexico City, Mexico; and Escuela Superior de  
Ingeniería Química e Industrias Extractivas  
Instituto Politécnico Nacional, UPALM  
Zacatenco, Mexico City Mexico

**Cristian Calderón**

Tecnológico de Monterrey, Mexico State  
Mexico

**Andrew Elyshev**

Tyumen State University, Tyumen, Russia

**Guillermo Félix**

Department of Petroleum Engineering  
Kazan Federal University, Kazan  
Russia and Tecnológico Nacional de  
México/IT de Los Mochis, Los Mochis  
Sinaloa, Mexico

**Nikita Glazov**

Boreskov Institute of Catalysis SB RAS  
Prospekt Akademika Lavrent'eva  
5, Novosibirsk, Novosibirsk Oblast  
Russian Federation

**Javier Jurado**

Instituto Politécnico Nacional, Centro de  
Investigación en Ciencia Aplicada y Tecnología  
Avanzada, Unidad Legaria, Legaria 694  
Col. Irrigación, Ciudad de México, Mexico

**Sergey Lopatin**

Boreskov Institute of Catalysis, Novosibirsk  
Russia and Tyumen State University  
Tyumen, Russia

**César I. Méndez**

Centro de Investigación en Ciencia Aplicada  
y Tecnología Avanzada del Instituto Politécnico  
Nacional, Mexico City, Mexico

**Alexis Tirado**

Department of Petroleum Engineering  
Kazan Federal University, Kazan, Russia

**Fernando Trejo**

Instituto Politécnico Nacional  
CICATA-Legaria, Ciudad de México, Mexico

**Andrey Zagoruiko**

Boreskov Institute of Catalysis, Novosibirsk  
Russia and Tyumen State University  
Tyumen, Russia

**Sergey Zazhigalov**

Boreskov Institute of Catalysis, Novosibirsk  
Russia and Tyumen State University  
Tyumen, Russia

**Vicente Samano**

Instituto Politécnico Nacional  
Centro de Investigación en Ciencia  
Aplicada y Tecnología Avanzada  
Unidad Legaria, Legaria 694  
Col. Irrigación  
Ciudad de México, Mexico



## Preface

After more than 30 years of experience working in the kinetic and reactor modeling of different processes for the petroleum and gas industry as well as for environmental protection applications, we have identified the need to have a collection of the most relevant cases that would have great impact on the industry. The general areas that are described in this book correspond to reaction kinetics, catalyst deactivation, reactor model, computational fluid dynamics, and steady-state and dynamics simulations using own experimental data or information reported in the literature.

*Mathematical Modeling of Complex Reaction Systems in the Oil and Gas Industry* is focused on the step-by-step description of kinetics and reactor modeling of various important processes used in the oil and gas industry. The topics covered in this book are hydrocracking of heavy oils, catalyst deactivation, oxidative regeneration of catalyst, adsorption–desorption catalytic processes, molecular reconstruction, production of green diesel via catalytic hydrotreating, slurry-phase hydrocracking reactor, Fischer–Tropsch synthesis and structured beds of micro-fibrous catalyst. Nowadays, all these topics are relevant to the oil and gas industry, particularly in this era of energy transition and decarbonization, which makes the book original and unique among previous reactor modeling books.

Each chapter describes the development of kinetic and reactor models for steady-state and dynamic simulations. To develop the kinetic model for each reaction or set of reaction for further reactor modeling, exhaustive experimental data either reported in the literature or generated in own laboratories are used. The developed models are validated with laboratory experimental data and simulation are reported to predict the commercial performance of the involved reactors. In addition, such a modeling in some cases allows for a deeper understanding of the qualitative essence of the phenomena observed in experiments, that is, to apply the augmented reality approach and make visible what cannot be directly observed in experiments, or at least to reproduce the most plausible picture of the physical events taking place.

This book is expected to be a reference guide for researchers, PhD students, postdoctoral researchers, catalyst manufacturers, process designers, and professors, to help them develop kinetic and reactor models at different reaction scales. It is also anticipated that this textbook can be used to cover part of the content of courses of different carriers at undergraduate and postgraduate levels.

*Jorge Ancheyta, National Polytechnic Institute and Mexican Institute of Petroleum, Mexico*

*Andrey Zagoruiko, Boreskov Institute of Catalysis, Novosibirsk, Russia*

*Andrey Elyshev, Tyumen State University, Russia*



## 1

## Modeling the Kinetics of Hydrocracking of Heavy Oil with Mineral Catalyst

Guillermo Félix<sup>1,2</sup>, Fernando Trejo<sup>3</sup>, and Jorge Ancheyta<sup>4,5</sup>

<sup>1</sup> Department of Petroleum Engineering, Kazan Federal University, Kazan, Russia

<sup>2</sup> Tecnológico Nacional de México/IT de Los Mochis, Los Mochis, Sinaloa, Mexico

<sup>3</sup> Instituto Politécnico Nacional, CICATA-Legaria, Legaria 694, Col. Irrigación, Ciudad de México, Mexico

<sup>4</sup> Instituto Mexicano del Petróleo, Eje Central Lázaro Cárdenas Norte 152, San Bartolo Atepehuacan, Mexico City, Mexico

<sup>5</sup> Escuela Superior de Ingeniería Química e Industrias Extractivas, Instituto Politécnico Nacional, UPALM, Zacatenco, Mexico City, Mexico

### 1.1 Introduction

The continuously increasing global demand for energy and the decrease of light crude oil reserves have caused researchers to look toward heavy crude oil reserves. Despite the importance of renewable sources is growing, fossil energy sources will continue to meet most of the global energy requirements (Bellussi et al. 2013; Félix and Ancheyta 2019a; Martínez-Grimaldo et al. 2014; Rana et al. 2007; Santos et al. 2014). The driving forces of the oil industries to improve heavy crude oils and vacuum residues (VRs) are as follows: (i) obtain high-quality transportation fuels, (ii) middle distillates, (iii) reduction of conventional crude oil supply, and (iv) price increase. Heavy crude oils or VRs are considered suitable alternative sources for transportation fuels, energy, and petrochemicals to meet the demands of industries. However, because of the low quality and difficulties in transporting heavy crude oils, it is necessary to develop technologies to upgrade their properties (Castañeda et al. 2014; Martínez-Grimaldo et al. 2014; Sahu et al. 2015).

In recent decades, researchers have prioritized refining techniques that use low-cost feedstock, such as coal, low-grade oil or wax, heavy crude oil, VRs, and natural gases, which are aimed to improve the cost-effectiveness of the refining process. The goal of these techniques is to transform such feedstock into transportation fuels and other low-boiling point liquid products. Refining heavy crude oils and VRs decreases their viscosity, initial boiling point, metal contents, sulfur, and other impurities, while increasing the  $H/C$  ratio to meet the commercial standards (Rodríguez et al. 2018; Sahu et al. 2015; Speight 2004).

#### 1.1.1 Reserves and Production of Heavy Crude Oils

The assessment of production capacity of oil field reveals that conventional light and medium oil reserves peaked in the 1960s. Since then, these reserves have steadily declined. An important focus of the global oil industry is to develop new technologies to be feasible: the use of unconventional resources as heavy and extra heavy crude oils (Heidary et al. 2017; Martínez et al. 2010; Santos et al. 2014). At the end of 2021, more than 1730 billion barrels of proven reserves are reported worldwide,

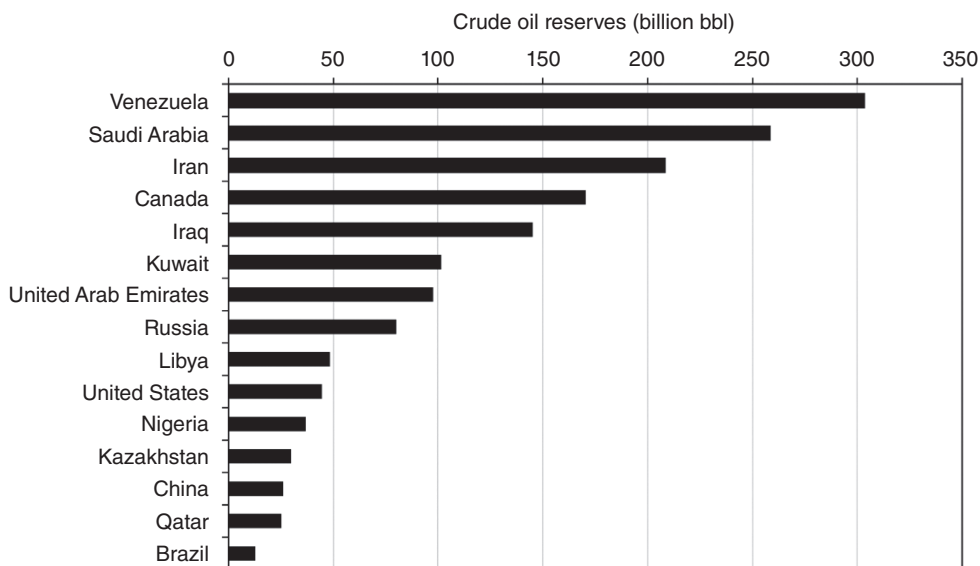


**Figure 1.1** Proven reserves of crude oil by country.

as shown in Figure 1.1 (*International—U.S. Energy Information Administration (EIA) 2021; Oil Gas Journal 2022; Organization of the Petroleum Exporting Countries (OPEC) 2020*). Venezuela, Saudi Arabia, and Iran possess the largest crude oil reserves; however, the quality of their crudes varies significantly. Currently, these reserves contain 434.3 billion barrels of heavy and extra-heavy crude oil, while 650.7 billion barrels correspond to bitumen, representing over 60% of the total volume (Bata et al. 2019; Pratama and Babadagli 2022).

### 1.1.2 Heavy Crude Oil Upgrading Processes

The processing of the heavy crude oil presents difficulties due to the complex nature of its heavier fractions, which commonly possess low API gravity (high density), high viscosity, elevated initial boiling point, higher contents of heteroatoms (sulfur, nitrogen, and oxygen), metals (Ni and V), and asphaltenes. In general, most of sulfur and nitrogen species present in crude oils are found in heavier fractions, while metals are found in porphyrins and as concentrated, exclusively in residue fractions (Ancheyta 2011; Memon et al. 2010; Qitian and Ancheyta 2016b). Therefore, the addition of hydrogen or rejection of carbon is the main process focused to increase the hydrogen-to-carbon ( $H/C$ ) ratio in heavy crudes. These two routes can be catalytic and noncatalytic (Ancheyta 2013; Félix et al. 2017).

Over the years, several technologies based on carbon rejection, the addition of hydrogen, and the combination of both have been used to upgrade heavy crude oils (Figure 1.2). The noncatalytic (deasphalting, gasification, coking, and visbreaking) and catalytic (catalytic cracking of VR) carbon rejection technologies account for 56.6% of the global processing technology due to its cost-effective operation. The noncatalytic (hydrovisbreaking) and catalytic (hydrotreating and hydrocracking) hydrogen addition technologies display advantages and disadvantages when applied to heavy crude oil processing as well as carbon rejection technologies (Castañeda et al. 2014; Rana et al. 2007; Sahu et al. 2015; Speight 2004).

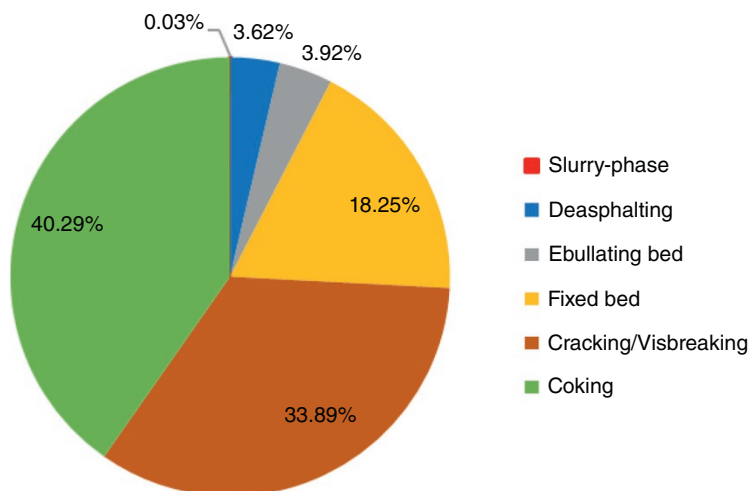


**Figure 1.2** Processing capacity for worldwide heavy crude oil upgrading technologies.

For heavy and extra-heavy crude oils, the choice between carbon rejection and hydrogen addition technologies depends on technical and economic assessments, as well as the quality of products from downstream refining processes. Therefore, deciding on which upgrading technology is appropriate for certain heavy crude oil is not an easy task and several factors must be taken into consideration, such as the following (Ancheyta 2013; Ancheyta and Speight 2007; Quitian and Ancheyta 2016b):

- ✓ Price of heavy crude oil
- ✓ Amount of impurities in feedstock
- ✓ Level of quality of the upgraded oil
- ✓ Process outline of the refinery

In the past, the carbon rejection technologies were preferred for feed with high metal content, such as heavy crude oils. Nonetheless, these technologies have the following disadvantages (Ancheyta 2013; Sahu et al. 2015):

- ✓ Low yield of upgraded oil
- ✓ Enhanced formation of coke
- ✓ High aromatic content in the upgraded oil
- ✓ Lower yield and quality of gasoline and diesel fuels
- ✓ Low value of upgraded oil

Technologies based on the hydrogen addition produce crude oils that possess superior quality and greater added value than carbon rejection methods do; hence, these approaches are becoming increasingly attractive. Highlights of the hydrogen addition technologies are the following:

- ✓ Minimizes the coke formation
- ✓ Enhances the yield of liquid products obtained by hydrocracking or hydrogenolysis mechanisms
- ✓ Increases the  $H/C$  ratio of the products
- ✓ Reduction of impurities, such as sulfur, nitrogen, metals, and asphaltenes
- ✓ Increases hydrogen consumption, giving higher liquid yields

These technologies also present the following disadvantages (Ancheyta 2013; Quitian and Ancheyta 2016b; Rana et al. 2007):

- ✓ Large volumes of hydrogen are necessary to carry out the hydrogenation of carbon-rich crude oil
- ✓ Difficulties arise from the carbon and metal deposition on the catalyst surface
- ✓ Requires well-designed catalysts that are able to process high levels of metals and asphaltenes within the feed

There are also some emerging technologies at different levels of development or even close to be commercialized, which have been developed due to the growing production of heavy and extra-heavy crude oils (Castañeda et al. 2014; Speight 2004). Hydrocracking is a well-known refining process where heavy crude oil in hydrogen atmosphere is transformed into light products with better quality. There are different types of reactors to carry out this process and the choice depends mainly on the level of conversion required and the number of impurities (metals and asphaltenes) in the feed. Three-phase catalytic reactors are highly valued due to their broad applications in various reaction systems and being notably used in the petroleum industry, including hydrocracking processes. Fixed-bed reactors have stable and reliable performance, but strong limitations are feed properties due to fast catalyst deactivation by coking and metal depositions. Ebullated-bed reactors perform better than fixed-bed reactors since they can process feed containing higher quantities of metals and coke at the expense to be conversion-limited and reaching values up to 80%. This is because of the rapid formation of sediments, by which commonly aromatic solvents are used to keep the soluble in the reacting phases. Slurry phase reactors achieve higher conversions performing superior levels of upgradation of feed rich in sulfur, metals, and asphaltenes (Ancheyta 2011; Jarullah et al. 2011; Martínez-Grimaldo et al. 2014; Sahu et al. 2015).

The degree of conversion is affected by the properties and nature of the feed, thus lighter crude oil possesses lower number of impurities, while heavy fractions contain higher content of asphaltenes (Alonso et al. 2019; Marafi et al. 2005; Ortega-García et al. 2012; Stanislaus et al. 2005; Stratiev et al. 2014, 2019; Tirado and Ancheyta 2018). Asphaltene is the most polar fraction found in heavy crudes and residues that is soluble in aromatic solvents but not in alkanes. This fraction comprises of both aromatic and aliphatic carbons, which contribute to its high molecular weight. The complex structure (Figure 1.3) makes asphaltenes one of the most studied fractions as they are coke precursors. The asphaltene fraction is formed by large aromatic sheets, side alkyl chains, heteroatoms, and metalloporphyrins. These latter components exhibit a remarkable influence of p-electronic interactions. The alteration in solubility during the processing of heavy crudes or residues is linked to solid formation. This disruption in solubility equilibrium relies on the chemical characteristics of the feed and the processing conditions. Based on the colloidal model (Figure 1.4), asphaltenes are surrounded by resin-building micelles keeping the asphaltenes dispersed in crude oil that avoids the contact with saturated compounds, since their nonpolar nature cause the instability of asphaltene micelles. Sediment formation is the result of a disturbance in the balance between asphaltenes and those compounds that keep them dispersed in solution during hydrotreating/hydrocracking; in other words, resins lose their peptization properties causing aggregation and precipitation of asphaltenes (Ashoori et al. 2017; Félix and Ancheyta 2019a; Ortega-García et al. 2012; Rana et al. 2007; Rogel et al. 2013; Stratiev et al. 2014, 2019; Tirado and Ancheyta 2018).

In addition to the loss of solubility of asphaltenes by oil and resin fractions, hydrocracking leads to an increase in the aromaticity and condensation of unconverted asphaltene cores. Reports indicate that the asphaltenes found in upgraded products have higher aromaticity and a lower  $H/C$  ratio in comparison with original asphaltenes in the feed. The results of structural analysis of the hexane-insoluble fraction indicate a higher degree of polarity due to the presence of a significant number of

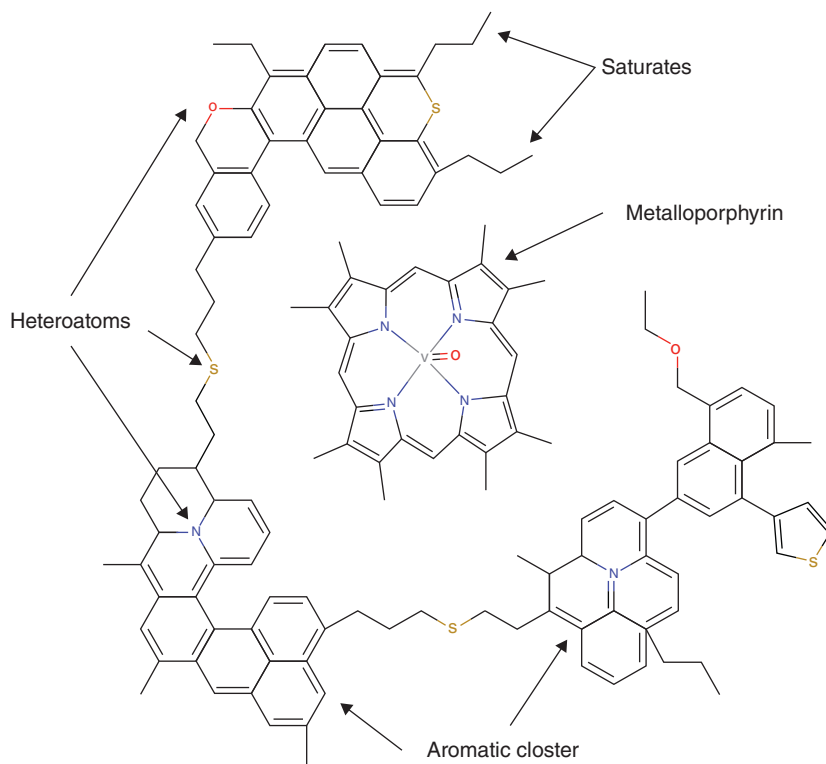


**Figure 1.3** Hypothetical asphaltene molecule.

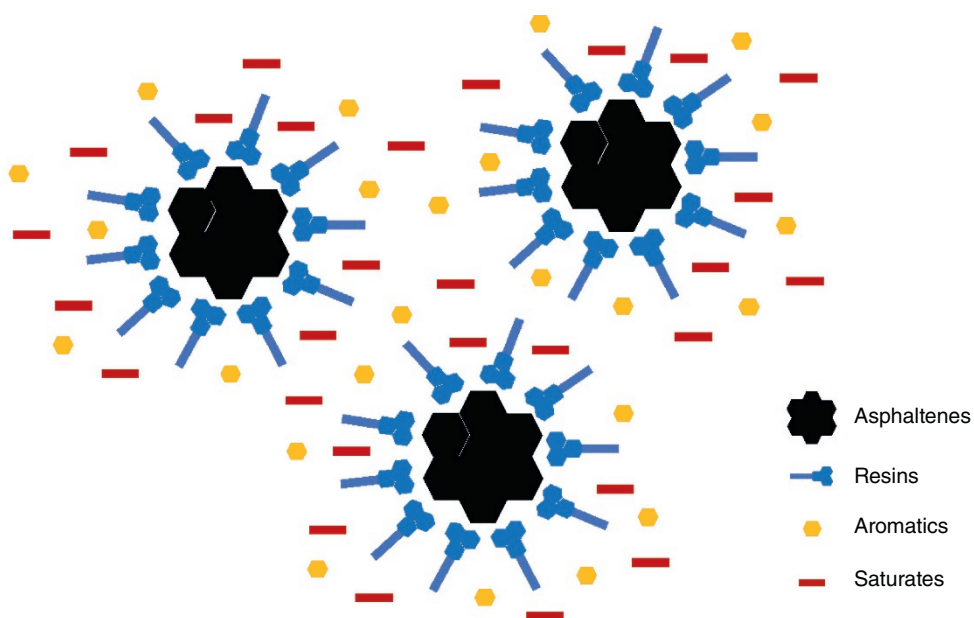


**Figure 1.4** Heavy crude oil composition based on SARA fractions.

heteroatoms with shorter alkyl chains because of the dealkylation reactions, which causes asphaltenes to become more aromatic and precipitate. The precipitation of sediment has also been attributed to the possible liquid–liquid phase separation of the material at high temperatures of processing (Mochida et al. 1989; Rogel et al. 2013; Tirado and Ancheyta 2018).

Sediment formation typically has a maximum limit of 0.8–1.0 wt.% in refineries. Higher values may cause commercial plants to shut down due to plugging issues. For this reason, sediment formation is a critical process parameter during hydrotreating and hydrocracking of heavy oils and thus dictates the maximum allowable residue conversion. Furthermore, a more extensive comprehension of sediment formation during upgrading processes is essential for enhancing both performance and control strategies. Improving the predictability of sediment deposition is highly desirable as it would enable the preliminary screening of feed and the optimization of processing (Alonso et al. 2019; Rogel et al. 2013; Tirado and Ancheyta 2018).

### 1.1.3 Reactions During Slurry Phase Hydrocracking

For hydrocracking reactions in slurry phase, the operating conditions can be classified as follows (Quitian and Ancheyta 2016a; Speight 2013):

- ❖ Mild conditions can be attained if the pressure and temperature do not exceed 80–100 kg/cm<sup>2</sup> and 410 °C, respectively, while the hydrocracking of heavy crude oil or residua leads to a VR of less than 50%.
- ❖ Severe conditions are reached at pressure and temperature exceeding 80–100 kg/cm<sup>2</sup> and 410 °C, respectively, and the VR conversion is greater than 50% during the hydrocracking of heavy crudes or residua.

Hydrocracking and hydrogenolysis are exothermic reactions and may occur at different extents depending on the operating conditions. At mild temperatures, hydrogenation is the dominant reaction unlike hydrocracking and thermal cracking reactions that take place at high temperatures (Quitian and Ancheyta 2016a; Raşeev 2003). The polyaromatic compounds break the weak bonds, such as C–S, C–O, and so on, and transform into free radicals. Meanwhile, the H<sub>2</sub> molecule dissociates to form Mo–H or S–H bonds, which in turn release hydrogen radicals to cap unstable compounds. Consequently, the formation and saturation of free radicals is a cyclic process. It has been reported that thermal and catalytic hydrocracking occur in series, the residue is converted to vacuum gas oil (VGO), medium distillate, naphtha, and gases, and the combination of thermal cracking and hydrogenation promotes the formation of the requested products (Martínez-Grimaldo et al. 2014; Nguyen et al. 2016; Quitian et al. 2015).

### 1.1.4 Catalysts for Hydrocracking of Heavy Crude Oils in Slurry Phase

The types of catalysts used in hydrocracking process are the solid heterogeneous powders and dispersed catalysts. The first type contains at least one metal (cobalt, molybdenum, nickel, iron) supported on alumina, silica–alumina, etc., by which the catalytic system is heterogeneous, containing the feed in liquid phase, the hydrogen in gaseous phase, and the catalyst in solid phase. As the reaction takes place, heavier molecules block the pore mouths and reduce the catalytic activity, thereby, reducing the reaction rate (Nguyen et al. 2016; Rodríguez et al. 2018). To solve this issue, unsupported catalysts were developed. The dispersed catalysts are particulate materials that enhance the catalytic hydrotreating at high reaction rates due to their large specific surface area, which makes the kinetics in the slurry phase faster than in fixed-, moving-, or ebullated-bed reactors. The faster

the mass and energy transfer, the lower the over-hydrocracking activity, and thereby, the lower the coke and gas formation (Liu et al. 2009; Quitian and Ancheyta 2016a).

Dispersed catalysts are highly stable by which optimized contact between oil and hydrogen is possible. As a result of high metal contents in dispersed catalysts, the heavy hydrocarbons reach the active sites very quickly and avoid plugging the pores as in supported catalysts. For these reasons, dispersed catalysts can be used directly in presence of heavier feedstock making slurry processes more suitable than other hydroconversion technologies when processing heavy feedstock (Angeles et al. 2014; Bellussi et al. 2013). Dispersed catalysts consist in different types: (i) soluble in water, (ii) soluble in oil (in this case heavy crude oil), (iii) mineral, and (iv) ionic liquid. The dispersed oil-soluble catalysts are generally more expensive than the water-soluble catalysts, but the water can evaporate during the reaction and reduce the catalytic activity, resulting in particle agglomeration. Meanwhile, the oil-soluble catalyst can be uniformly dispersed in the feed enhancing hydrogen uptake and suppressing the coke formation. The conversion as well as the quality of liquid product increases (Galarraga et al. 2012; Kim et al. 2017; Liu et al. 2009; Nguyen et al. 2016).

The mineral catalysts are natural ores with a high content of one or more transition metals, usually the Fe-based and Mo-based minerals are the most employed for slurry-phase hydrocracking. Different works have been employed magnetite, limonite, hematite, ferrite, laterite, pyrite, and molybdenite, among others. This type of catalyst does not require any special preparation, instead drying, grinding, and sieving are the usual operations required before using, making them cheaper than other catalysts (Al-Attas et al. 2019; Fukuyama and Terai 2007; Quitian and Ancheyta 2017). The ionic liquid catalysts are a relatively new alternative to dispersed catalysts. These compounds are organic salts that can be liquefied at near room temperature. Their catalytic activity depends primarily on the cations and anions used during synthesis and usually contain molybdenum, cobalt, iron, or nickel (Cai et al. 2022; Ma et al. 2022). It is preferred to use molybdenum compounds as dispersed catalysts due to their greater hydrogenation activity (Calderon and Ancheyta 2016; Du et al. 2015; Panariti et al. 2000). It has been shown that metal sulfide is the active species in hydrocracking process, and it is formed by reacting the metal precursors with sulfur compounds in the feed or additional sources of sulfur (Nguyen et al. 2016; Panariti et al. 2000). The sulfidation (activation of catalysts) is done before the hydrocracking reaction and starts by two routes: (i) *ex situ* and (ii) *in situ* sulfidation. In the case of *ex situ* sulfidation, the sulfur sources are often found in carbonaceous compounds (as heavy crude oils) or using hydrogen sulfide (Nguyen et al. 2016; Quitian and Ancheyta 2016a). Small concentration of low-cost, finely dispersed catalyst makes recovery impractical after reaction. In addition, slurry catalysts are deactivated after reaction, which occurs by coke and metal deposition hindering its reuse (Quitian and Ancheyta 2016a; Rezaei 2013).

## 1.2 Kinetic Models

For adequate modeling of a new hydrocracking process is imperative to take into account the feed properties, design, performance, process control, and cost to meet the specification of the products. The main issue when modeling hydrocracking process is the complex nature of feedstock compared with model compounds by which it is necessary to understand the changes in the rate constants, conversion, and API gravity at different reaction scales. This will improve the methodologies for upscaling reaction parameters from the laboratory to industrial scale (Ancheyta et al. 2005; Becker et al. 2016; Celse et al. 2015; Elizalde et al. 2009; Hassanzadeh and Abedi 2010; Marafi et al. 2010; Rashidzadeh et al. 2011).

### 1.2.1 General Types of Kinetic Models

Discrete and continuous lumping models have been largely used to represent the reaction kinetics. Recently, the use of more complex and fundamental microkinetic models to simulate hydrocracking has increased the interest of the research community (Becker et al. 2016; Martínez and Ancheyta 2012; Sánchez et al. 2005a). The yield of gases, naphtha, middle distillates, VGO, and residue based on boiling point intervals is adequately predicted by kinetic models. In addition, the so-called SARA fractions, that is, saturates, aromatics, resins, and asphaltenes, are also included in the modeling. Kinetic studies for the transformation of asphaltenes into maltenes fractions (saturates, aromatics, and resins) have received less attention than those involving the pseudocomponents based on boiling point ranges (Asaee et al. 2014; Félix and Ancheyta 2019a; Moustafa and Froment 2003).

#### 1.2.1.1 Lumping Kinetic Models

Traditional models by pseudocomponents take macroscopic properties (for example, measurable properties in the product) and derive the equation system to be solved. These models can be specifically grouped into compounds in the feed or products in a few cuts, often characterized by ranges of boiling points that undergo different reactions in series or parallel (Ancheyta 2013; Ancheyta et al. 2005; Balasubramanian and Pushpavanam 2008; Elizalde et al. 2009; Galarraga et al. 2012; Hassanzadeh and Abedi 2010; Moghadassi et al. 2011).

Models based on pseudocomponents (up to 10) are commonly reported in the literature to simplify the large number of hydrocarbons present in heavy crude oil fractions for lumping purposes during hydrocracking. These models are used to simulate the yield of fractions of interest for refiners or process designers in spite of the reduced amount of information obtained from pseudocomponent-based models. When a distillation curve is required, a small number of pseudocomponents must be interpolated, while the number of kinetic parameters to be calculated increases exponentially, which clearly is not feasible when modeling (Asaee et al. 2014; Becker et al. 2016; Quitian and Ancheyta 2016a; Sadighi et al. 2010).

#### 1.2.1.2 Continuous Lumping Kinetic Models

Continuous models overcome limitations in lumping models by considering that petroleum is formed by an infinite number of components, allowing crude to be considered as a continuous mixture instead of pseudocomponents. Continuous mixing takes into account a large number of undefined species contained in the oil fraction, and the difference between adjacent species is relatively smaller (Ancheyta 2013; Elizalde et al. 2009).

A continuous function describes the reactivity, while the distillation curve is considered to solve the model keeping the number of parameters constant. In addition, properties, such as the carbon number or the true boiling points in distillation, are used to characterize the feedstock and products in the continuous kinetic modeling. The combination of continuous models and pseudocomponents allows more than one continuous distribution to be obtained. However, this model is highly depending on feed properties, and its advantages are as follows (Ancheyta 2013; Becker et al. 2016):

- ✓ Prediction of the distillation curve with few parameters to be estimated
- ✓ Track the chemistry of the process accurately
- ✓ Individual reaction order has physical meaning
- ✓ The properties of fractions between the initial and final boiling points are easily obtained
- ✓ The heteroatom distribution curve is well predicted
- ✓ Easy to adapt to heavy, extra-heavy crudes and residue kinetics

The model involves the dimensionless temperature ( $\theta$ ) and weight fraction, which is calculated as follows:

$$\theta = \frac{\text{TBP} - \text{TBP}(l)}{\text{TBP}(h) - \text{TBP}(l)} \quad (1.1)$$

where TBP is the true boiling point temperature (in kelvin) of any component, TBP(h) and TBP(l) are the highest and lowest boiling points in the mixture, respectively. Because the TBP of the distillation curve is a function of the reactivity ( $\lambda$ ), a coordinate transformation between discrete and continuous forms (from the TBP to reactivity for any mixture) is expressed as follows:

$$\frac{\lambda}{\lambda_{\max}} = \theta^{\frac{1}{\alpha}} \quad (1.2)$$

where  $\lambda_{\max}$  and  $\alpha$  are positive constants and model parameters;  $\lambda_{\max}$  is the reactivity for species with the highest dimensionless temperature. The distribution function of species type ( $D(\lambda)$ ) is necessary to transform the coordinates adequately from  $\theta$  to  $\lambda$ , and it is defined as follows:

$$D(\lambda) = \frac{n_s \alpha}{\lambda_{\max}^{\alpha}} \lambda^{\alpha-1} \quad (1.3)$$

where  $n_s$  is the total number of species in the mixture. The equation of mass balance as a function of the reactivity and residence time ( $t$  or  $\text{LHSV}^{-1}$ ) after changing the coordinates, becomes

$$\frac{dc(\lambda, t)}{dt} = -\lambda c(\lambda, t) + \int_{\lambda}^{\lambda_{\max}} p(\lambda, \Lambda) \Lambda c(\Lambda, t) D(\Lambda) d\Lambda \quad (1.4)$$

where  $c(\lambda, t)$  is the concentration of the component with reactivity  $\lambda$ ,  $c(\Lambda, t)$  is the concentration of the component with reactivity  $\Lambda$ ,  $p(\lambda, \Lambda)$  is the probability density function of species with reactivity  $\Lambda$  that can form species with reactivity  $\lambda$ ,  $\Lambda$  is the maximum reactivity of the same component with reactivity  $\lambda$ , and  $D(\Lambda)$  is the Jacobian that transforms the discrete coordinate  $i$  into a continuous coordinate  $\Lambda$ . The form of the function  $p(\lambda, \Lambda)$  and its parameters are given by:

$$p(\lambda, \Lambda) = \frac{1}{S_0 \sqrt{2\pi}} \left[ e^{-\left( \frac{\{[\lambda]^{a_0 - 0.5}\}}{a_1} \right)^2} - A_1 + B_1 \right] \quad (1.5)$$

$$A_1 = e^{-\left( \frac{0.5}{a_1} \right)^2} \quad (1.6)$$

$$B_1 = \sigma \left[ 1 - \left( \frac{\lambda}{\Lambda} \right) \right] \quad (1.7)$$

where  $a_0$ ,  $a_1$ , and  $\sigma$  are parameters of the model, and  $S_0$  is obtained from the following mass balance criteria:

$$\int_0^{\Lambda} p(\lambda, \Lambda) D(\lambda) d\lambda = 1 \quad (1.8)$$

where  $D(\lambda)$  is the Jacobian that transforms the discrete coordinate  $i$  into the continuous coordinate  $\lambda$ . Using this equation and solving Eq. (1.5) to  $S_0$ , the following solution is reached:

$$S_0 = \int_0^{\Lambda} \frac{1}{\sqrt{2\pi}} \left[ e^{-\left( \frac{\{[\lambda]^{a_0 - 0.5}\}}{a_1} \right)^2} - A_1 + B_1 \right] D(\lambda) d\lambda \quad (1.9)$$

The hydrocracking phenomena occurring within the reactor are described by the differential equation, which illustrates the formation of compounds resulting from the cracking of components with higher boiling points (second term on the right side of the equation) and the cracking of lower boiling products (first term of the equation). This equation is solved for any residence time in terms of  $c(\lambda, t)$ , and the desired cuts in mass fraction depending on its dimensionless temperature as follows:

$$C_{\theta_1, \theta_2}(t) = \int_{\lambda_1}^{\lambda_2} c(\lambda, t) D(\lambda) d\lambda \quad (1.10)$$

where  $C_{\theta_1, \theta_2}(t)$  is the mass fraction with dimensionless temperature ranging from  $\theta_1$  to  $\theta_2$  with its corresponding reactivity  $\lambda_1$  and  $\lambda_2$  as shown in Eq. (1.2) (Ancheyta 2013; Becker et al. 2016; Elizalde et al. 2009, 2016; Elizalde and Ancheyta 2014; Laxminarasimhan et al. 1996; Martínez-Grimaldo et al. 2011).

### 1.2.1.3 Single-Event Kinetic Models

Microkinetic models are developed at a molecular scale considering the chemistry of the reaction system by deriving the kinetic equations for individual molecules. The solution adequately converges in reacting systems that contain a limited number of chemical species. However, the set of equations suggested for intricate systems, such as those represented by heavy crude fractions, presents a challenging task to accomplish. Even modern computational tools are unsatisfactory because the size of the reaction network increases exponentially with the number of carbons (Ancheyta et al. 2005; Becker et al. 2016).

The advancement of these types of models for hydrocracking of heavy crude oils is propelled by the rising availability of experimental data gathered using sophisticated analytical techniques and increasing computational capacities. The microkinetic modeling method (single events) was initially proposed by Froment et al. (Baltanas et al. 1989; Baltanas and Froment 1985; Froment 1987; Hillewaert et al. 1988), and the reaction coefficients were calculated for each individual reaction. Computational regrouping algorithms reduce the size of reaction networks without losing information. These can be applied in various reactions, such as hydrocracking, catalytic reformation, isomerization and alkylation; however, the original regrouping method remains as unsuitable for implementation in huge network of reactions, notwithstanding the current computational capabilities. To find an approach, two alternative methods have been proposed (Becker et al. 2016; Guillaume et al. 2011; Mitsios et al. 2009; Valéry et al. 2007): (i) a method based on decomposition of side chains that was developed by Valéry et al. (2007) and (ii) a method based on structural classes, which was developed by Martens and Marin (2001).

## 1.2.2 Kinetic Models Reported in the Literature for Hydrocracking of Heavy Crude Oils Using Dispersed Catalysts

### 1.2.2.1 Kinetic Models Based on Distillation Curves

Hassanzadeh and Abedi (2010) as well as Galarraga et al. (2012) carried out experiments for the catalytic heavy crude oil upgrading with dispersed NiWMo catalyst and Athabasca bitumen (9.5 °API) as feed in a batch reactor. The tests were performed at temperature ranges of 320–380 °C, 3–70 h of reaction time, total hydrogen pressure of 3.45 MPa, and stirring rate of 500 rpm. Both works used the same kinetic model (Figure 1.5a) that was first reported by Sánchez et al. (2005a) based on boiling point intervals. The reaction scheme takes into account five lumps: Residue (R, 538 °C+), VGO (343–538 °C), distillates (D, 204–343 °C), naphtha (N, IBP–204 °C), and

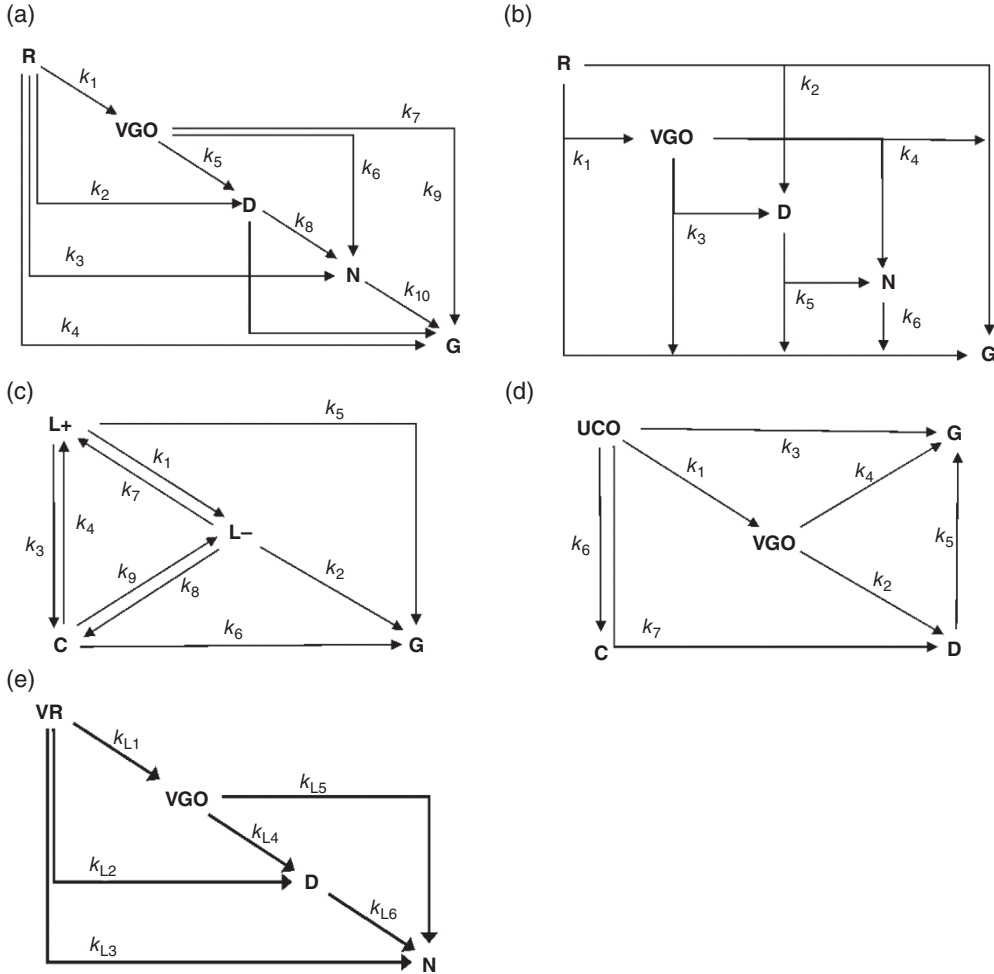


**Figure 1.5** Four- and five-lump kinetic models based on distillation curves reported in the literature for heavy oil hydrocracking using dispersed catalyst.

gases (G). Nonetheless, some pseudocomponents proposed by Galarraga et al. (2012) have different boiling point ranges: residue (545 °C+), VGO (343–545 °C), D (216–343 °C), N (IBP–216 °C). The mass balance equations are the same in both cases, and a first-order reaction was considered giving the following expressions:

$$r_R = -(k_1 + k_2 + k_3 + k_4)y_R \quad (1.11)$$

$$r_{VGO} = k_1y_R - (k_5 + k_6 + k_7)y_{VGO} \quad (1.12)$$

$$r_D = k_2y_R + k_5y_{VGO} - (k_8 + k_9)y_D \quad (1.13)$$

$$r_N = k_3y_R + k_6y_{VGO} + k_8y_D - k_{10}y_N \quad (1.14)$$

$$r_G = k_4y_R + k_7y_{VGO} + k_9y_D + k_{10}y_N \quad (1.15)$$

where  $r_i$  is the reaction rate of the component  $i$ ,  $y_i$  the mass fractions of component  $i$ ,  $k_j$  the reaction rate coefficients for each reaction pathway  $j$ . The only difference is that Hassanzadeh and Abedi

(2010) used the weight fraction, while Galarraga et al. (2012) employed a dimensionless concentration (the concentration at any time divided by the initial concentration). Furthermore, the latter authors performed a general reaction for the residue conversion into light products assuming first-order reaction with  $k_0$  as the only reaction rate coefficient as follows:



After the catalytic hydrocracking of Athabasca bitumen with ultradispersed catalyst at bench-scale, kinetic studies on a large-scale reactor were developed by Loria et al. (2011) using the same model as Galarraga et al. (2012). The experimental results were obtained in a pilot plant tubular reactor at reaction temperatures of 320–380 °C, residence times ( $\tau$ , for continuous reactors is assumed to be the ratio of the reactor volume to the volumetric flow rate) of 9–51 h, keeping the total pressure constant (2.76 MPa), and a hydrogen-to-oil ratio of 3509 (scf/bbl). Although the reaction scheme is the same, some boiling point intervals are different: VGO (343–550 °C) and R (550 °C+). Because an ultradispersed catalyst is employed in the study, the internal and external diffusion and the axial dispersion were negligible in a continuous gas-oil hydrocracking reactor, which allowed to set the reaction equations as follows:

$$\int_{y(\tau_0)}^{y(\tau_f)} dy_R = -k_1 \int_{\tau_0}^{\tau_f} y_R d\tau - k_2 \int_{\tau_0}^{\tau_f} y_R d\tau - k_3 \int_{\tau_0}^{\tau_f} y_R d\tau - k_4 \int_{\tau_0}^{\tau_f} y_R d\tau \quad (1.17)$$

$$\int_{y(\tau_0)}^{y(\tau_f)} dy_{VGO} = k_1 \int_{\tau_0}^{\tau_f} y_R d\tau - k_5 \int_{\tau_0}^{\tau_f} y d\tau - k_6 \int_{\tau_0}^{\tau_f} y_{VGO} d\tau - k_7 \int_{\tau_0}^{\tau_f} y_{VGO} d\tau \quad (1.18)$$

$$\int_{y(\tau_0)}^{y(\tau_f)} dy_D = k_2 \int_{\tau_0}^{\tau_f} y_R d\tau + k_5 \int_{\tau_0}^{\tau_f} y_{VGO} d\tau - k_8 \int_{\tau_0}^{\tau_f} y_D d\tau - k_9 \int_{\tau_0}^{\tau_f} y_D d\tau \quad (1.19)$$

$$\int_{y(\tau_0)}^{y(\tau_f)} dy_N = k_3 \int_{\tau_0}^{\tau_f} y_R d\tau + k_6 \int_{\tau_0}^{\tau_f} y_{VGO} d\tau + k_8 \int_{\tau_0}^{\tau_f} y_D d\tau - k_{10} \int_{\tau_0}^{\tau_f} y_N d\tau \quad (1.20)$$

$$\int_{y(\tau_0)}^{y(\tau_f)} dy_G = k_4 \int_{\tau_0}^{\tau_f} y_R d\tau + k_7 \int_{\tau_0}^{\tau_f} y_{VGO} d\tau + k_9 \int_{\tau_0}^{\tau_f} y_D d\tau + k_{10} \int_{\tau_0}^{\tau_f} y_N d\tau \quad (1.21)$$

where  $\tau_0$  and  $\tau_f$  are the initial and final residence times, respectively, and  $y(\tau_0)$  and  $y(\tau_f)$  are the initial and final weight percentages, respectively, as a function of the residence time.

Nguyen et al. (2013) carried out a kinetic study for the hydrocracking of the Arabian light atmospheric residue in a batch reactor using Mo-dispersed catalyst (molybdenum naphthenate). The experiments were carried out at temperatures of 420–430 °C, residence times of 0.5–1 h, and hydrogen pressure of 15.2 MPa. The proposed reaction scheme (Figure 1.5b) considered the following boiling point intervals: R (510 °C+), VGO (350–510 °C), D (180–350 °C), and N (IBP–180 °C). A first order was assumed for all the reactions and the reaction from R to N was neglected;